

**FIG. 5.** (A) ABR threshold (mean  $\pm$  SD) at each frequency tested preoperatively (pre) versus postoperatively (post). (B) Example of ABR waveforms in C57BL/6j at various stimuli (16 kHz; 108 dB, 78 dB, 48 dB, 28 dB, and 23 dB). ABR were tested in the transduced ear prior to viral injection and 10 days after injection. Wave I was measured to analyze the activity of the cochlea. (C) F-actin staining showing that no outer hair cells were lost from inoculated cochleae. Original magnification 40 $\times$ ; scale bar, 25  $\mu$ m.

gradient as described previously [24]. The viral stock was treated with DNase and titrated by quantitative real-time PCR with plasmid standards [43].

**Surgical procedures and cochlear perfusions.** All animal studies were performed in accordance with the guidelines issued by the committee on animal research of Jichi Medical School and approved by its ethics

committee. Sixty female C57BL/6J mice (4 weeks of age; CLEA Japan, Tokyo, Japan) and 40 male ICR mice (2 months of age; Japan SLC, Shizuoka, Japan) were utilized. The mice were initially anesthetized with ketamine (50 mg/kg) and the analgesic xylazine (5 mg/kg). A postauricular approach was used to expose the tympanic bony bulla. A small opening (2 mm) in the tympanic bulla was carefully made to allow access to the round window membrane. In the tested groups, 5  $\mu$ l AAV vector solution ( $5 \times 10^{10}$  gc) was microinjected into the cochlea through the round window over 10 min with a glass micropipette (40  $\mu$ m in diameter) fitted on a Univentor 801 syringe pump (Serial No. 170182, High Precision Instruments, Univentor Ltd., Malta) [19]. A small plug of muscle was used to seal the cochlea and the surgical wound was closed in layers and dressed with antibiotic ointment. Five mice of each strain received control cochlear perfusions with artificial perilymph (145 mM NaCl, 2.7 mM KCl, 2 mM MgSO<sub>4</sub>, 1.2 mM CaCl<sub>2</sub>, 5 mM Hepes) alone. Each AAV-EGFP serotype was injected into five mice of each strain. Another 20 C57BL/6J mice were injected with the AAV3 vector to study long-term expression.

**Cochlear function assessment using ABR.** To assess the physiological status of experimental ears, auditory thresholds were determined with multiple frequency and intensity tone bursts by performing ABR audiometry with Tucker-Davis Technologies and Scope v3.6.9 software (Power Lab/200; ADInstruments, Castle Hill, Australia). Tone pipes were introduced into the operated ears of the anesthetized mice, and evoked potentials were recorded using needle electrodes inserted through the skin. ABR were elicited and measured 256 times at 4, 8, 12, 16, 20, and 24 kHz frequencies with tone bursts in systematic 5-dB steps. The rise/fall times for the tone bursts were 0.1 ms rise/ms flat (cosine gate). Free-field system was used as a calibration procedure. Wave I was measured to analyze the activity from the cochlea. The lowest stimulus level that yielded a detectable ABR waveform was defined as the threshold. ABR were tested in the infused ear prior to surgery and 10 days postsurgery. Data were statistically analyzed using repeated-measures analysis of variance followed by paired Student's *t* test performed with StatView 5.0 software (SAS Institute Inc., Cary, NC, USA). Values of *P* < 0.05 were considered significant.

**Histology.** Cochlear transgene expression patterns were determined for all AAV serotypes by visualizing EGFP expression. The animals were sacrificed 10 days after injection, and intracardiac perfusion was performed with 4% paraformaldehyde (PFA) in 0.1 M phosphate buffer, pH 7.4. The cochleae were harvested and the stapes footplates were removed. For AAV3-mediated transduction, the animals (five mice for each time point) were sacrificed 1, 2, 4, 8, or 12 weeks after inoculation. Postfixation was carried out in 4% PFA for 4 h at 4°C, and decalcification was performed in 10% EDTA for 12 days at room temperature. The cochlear half-turns were microdissected and processed and the other half-turns were prepared by cryosection (10  $\mu$ m) to detect EGFP expression by using an Olympus IX70 (Olympus Corp., Tokyo, Japan) fluorescence microscope with a standard fluorescein isothiocyanate filter set and Studio Lite software (Olympus Corp.). Cells that exhibited fluorescence were considered positive for transgene expression. The level of expression was graded by fluorescence intensity on a four-point scale (+, ++, +++, +++) depending on the pixel/unit area count. Hair cell counts were carried out with dissected cochlea.

#### ACKNOWLEDGMENTS

The authors thank Avigen, Inc. (Alameda, CA, USA) for providing pAAV-LacZ, pHLP19, and pAdeno; Dr. John A. Chiorini for pAAV4RepCap (identical to pSV40oriAAV4-2), pAAV5-RNL, and pAAV5RepCap (identical to SRepCapB); and Dr. James M. Wilson for pAAV7RepCap and pAAV8RepCap. We also thank Dr. John E. Donello (Infectious Disease Laboratory, The Salk Institute for Biological Studies) for providing pBS II SK<sup>+</sup>WPRE-B11 and Dr. Jun-Ichi Miyazaki (Osaka University Graduate School of Medicine) for pCAGGS. The authors also thank Mr. Takeshi Hayakawa (Bio Research Center Co., Ltd.), Ms. Miyoko Mitsu, and Ms. Kiyomi Aoki for their encouragement and technical support. This study was supported in part by (1) grants from the Ministry of Health, Labor, and Welfare of Japan; (2) Grants-in-Aid for Scientific Research;

(3) a grant from the 21 Century COE Program; and (4) the High-Tech Research Center Project for Private Universities matching fund subsidy from the Ministry of Education, Culture, Sports, Science, and Technology of Japan.

RECEIVED FOR PUBLICATION NOVEMBER 1, 2004; ACCEPTED MARCH 24, 2005.

#### REFERENCES

- Raphael, Y., Frisnacho, J. C., and Roessler, B. J. (1996). Adenoviral-mediated gene transfer into guinea pig cochlear cells in vivo. *Neurosci. Lett.* 207: 137–141.
- Holt, J. R., et al. (1999). Functional expression of exogenous proteins in mammalian sensory hair cells infected with adenoviral vectors. *J. Neurophysiol.* 81: 1881–1888.
- Yamasoba, T., Suzuki, M., and Kondo, K. (2002). Transgene expression in mature guinea pig cochlear cells in vitro. *Neurosci. Lett.* 335: 13–16.
- Derby, M. L., Sena-Esteves, M., Breakefield, X. O., and Corey, D. P. (1999). Gene transfer into the mammalian inner ear using HSV-1 and vaccinia virus vectors. *Hear. Res.* 134: 1–8.
- Chen, X., Frisina, R. D., Bowers, W. J., Frisina, D. R., and Federoff, H. J. (2001). HSV amplicon-mediated neurotrophin-3 expression protects murine spiral ganglion neurons from cisplatin-induced damage. *Mol. Ther.* 3: 958–963.
- Bowers, W. J., Chen, X., Guo, H., Frisina, D. R., Federoff, H. J., and Frisina, R. D. (2002). Neurotrophin-3 transduction attenuates cisplatin spiral ganglion neuron ototoxicity in the cochlea. *Mol. Ther.* 6: 12–18.
- Han, J. J., et al. (1999). Transgene expression in the guinea pig cochlea mediated by a lentivirus-derived gene transfer vector. *Hum. Gene Ther.* 10: 1867–1873.
- Lalwani, A. K., Walsh, B. J., Reilly, P. G., Muzyczka, N., and Mhatre, A. N. (1996). Development of in vivo gene therapy for hearing disorders: introduction of adeno-associated virus into the cochlea of the guinea pig. *Gene Ther.* 3: 588–592.
- Lalwani, A., et al. (1998). Long-term in vivo cochlear transgene expression mediated by recombinant adeno-associated virus. *Gene Ther.* 5: 277–281.
- Luebke, A. E., Foster, P. K., Muller, C. D., and Peel, A. L. (2001). Cochlear function and transgene expression in the guinea pig cochlea, using adenovirus- and adeno-associated virus-directed gene transfer. *Hum. Gene Ther.* 12: 773–781.
- Luebke, A. E., Steiger, J. D., Hodges, B. L., and Amalfitano, A. (2001). A modified adenovirus can transfect cochlear hair cells in vivo without compromising cochlear function. *Gene Ther.* 8: 789–794.
- Staecker, H., Li, D., O'Malley, B. W., Jr., and Van De Water, T. R. (2001). Gene expression in the mammalian cochlea: a study of multiple vector systems. *Acta Otolaryngol.* 121: 157–163.
- Dazerf, S., Aletsee, C., Brors, D., Gravel, C., Sendtner, M., and Ryan, A. (2001). In vivo adenoviral transduction of the neonatal rat cochlea and middle ear. *Hear. Res.* 151: 30–40.
- Ishimoto, S., Kawamoto, K., Kanzaki, S., and Raphael, Y. (2002). Gene transfer into supporting cells of the organ of Corti. *Hear. Res.* 173: 187–197.
- Van de Water, T. R., Staecker, H., Halterman, M. W., and Federoff, H. J. (1999). Gene therapy in the inner ear: mechanisms and clinical implications. *Ann. N.Y. Acad. Sci.* 884: 345–360.
- Vassalli, G., Bueler, H., Dudler, J., von Segesser, L. K., and Kappenberger, L. (2003). Adeno-associated virus (AAV) vectors achieve prolonged transgene expression in mouse myocardium and arteries in vivo: a comparative study with adenovirus vectors. *Int. J. Cardiol.* 90: 229–238.
- Li Duan, M., Bordet, T., Mezzina, M., Kahn, A., and Ulfendahl, M. (2002). Adenoviral and adeno-associated viral vector mediated gene transfer in the guinea pig cochlea. *Neuroreport* 13: 1295–1299.
- Lalwani, A. K., Han, J. J., Walsh, B. J., Zolotukhin, S., Muzyczka, N., and Mhatre, A. N. (1997). Green fluorescent protein as a reporter for gene transfer studies in the cochlea. *Hear. Res.* 114: 139–147.
- Kho, S. T., Pettis, R. M., Mhatre, A. N., and Lalwani, A. K. (2000). Cochlear microinjection and its effects upon auditory function in the guinea pig. *Eur. Arch. Otorhinolaryngol.* 257: 469–472.
- Handa, A., Muramatsu, S., Qiu, J., Mizukami, H., and Brown, K. E. (2000). Adeno-associated virus (AAV)-3-based vectors transduce haematopoietic cells not susceptible to transduction with AAV-2-based vectors. *J. Gen. Virol.* 81: 2077–2084.
- Davidson, B. L., et al. (2000). Recombinant adeno-associated virus type 2, 4, and 5 vectors: transduction of variant cell types and regions in the mammalian central nervous system. *Proc. Natl. Acad. Sci. USA* 97: 3428–3432.
- Zabner, J., et al. (2000). Adeno-associated virus type 5 (AAV5) but not AAV2 binds to the apical surfaces of airway epithelia and facilitates gene transfer. *J. Virol.* 74: 3852–3858.
- Yang, G. S., et al. (2002). Virus-mediated transduction of murine retina with adeno-associated virus: effects of viral capsid and genome size. *J. Virol.* 76: 7651–7660.
- Okada, T., et al. (2002). Adeno-associated virus vectors for gene transfer to the brain. *Methods* 28: 237–247.
- Xu, L., et al. (2001). CMV-beta-actin promoter directs higher expression from an

- adeno-associated viral vector in the liver than the cytomegalovirus or elongation factor 1 alpha promoter and results in therapeutic levels of human factor X in mice. *Hum. Gene Ther.* 12: 563–573.
26. Chung, S., Andersson, T., Sonntag, K. C., Bjorklund, L., Isacson, O., and Kim, K. S. (2002). Analysis of different promoter systems for efficient transgene expression in mouse embryonic stem cell lines. *Stem Cells* 20: 139–145.
  27. Nomoto, T., et al. (2003). Distinct patterns of gene transfer to gerbil hippocampus with recombinant adeno-associated virus type 2 and 5. *Neurosci. Lett.* 340: 153–157.
  28. Dutta, S. K. (1975). Isolation and characterization of an adenovirus and isolation of its adenovirus-associated virus in cell culture from foals with respiratory tract disease. *Am. J. Vet. Res.* 36: 247–250.
  29. Palmer, E., and Goldsmith, C. S. (1988). Ultrastructure of human retroviruses. *J. Electron Microsc. Tech.* 8: 3–15.
  30. Stover, T., Yagi, M., and Raphael, Y. (1999). Cochlear gene transfer: round window versus cochleostomy inoculation. *Hear. Res.* 136: 124–130.
  31. Stover, T., Yagi, M., and Raphael, Y. (2000). Transduction of the contralateral ear after adenovirus-mediated cochlear gene transfer: round window versus cochleostomy inoculation. *Gene Ther.* 7: 377–383.
  32. Kawamoto, K., Oh, S. H., Kanzaki, S., Brown, N., and Raphael, Y. (2001). The functional and structural outcome of inner ear gene transfer via the vestibular and cochlear fluids in mice. *Mol. Ther.* 4: 575–585.
  33. Kaplitt, M. G., et al. (1994). Long-term gene expression and phenotypic correction using adeno-associated virus vectors in the mammalian brain. *Nat. Genet.* 8: 148–154.
  34. Okada, T., et al. (2001). Development and characterization of an antisense-mediated prepackaging cell line for adeno-associated virus vector production. *Biochem. Biophys. Res. Commun.* 288: 62–68.
  35. Chiorini, J. A., Kim, F., Yang, L., and Kotin, R. M. (1999). Cloning and characterization of adeno-associated virus type 5. *J. Virol.* 73: 1309–1319.
  36. Zufferey, R., Donello, J. E., Trono, D., and Hope, T. J. (1999). Woodchuck hepatitis virus posttranscriptional regulatory element enhances expression of transgenes delivered by retroviral vectors. *J. Virol.* 73: 2886–2892.
  37. Matsushita, T., et al. (1998). Adeno-associated virus vectors can be efficiently produced without helper virus. *Gene Ther.* 5: 938–945.
  38. Mochizuki, S., et al. (2004). Adeno-associated virus (AAV) vector-mediated liver- and muscle-directed transgene expression using various kinds of promoters and serotypes. *Gene Ther. Mol. Biol.* 8: 9–18.
  39. Muramatsu, S., Mizukami, H., Young, N. S., and Brown, K. E. (1996). Nucleotide sequencing and generation of an infectious clone of adeno-associated virus 3. *Virology* 221: 208–217.
  40. Chiorini, J. A., Yang, L., Liu, Y., Safer, B., and Kotin, R. M. (1997). Cloning of adeno-associated virus type 4 (AAV4) and generation of recombinant AAV4 particles. *J. Virol.* 71: 6823–6833.
  41. Gao, G. P., Alvira, M. R., Wang, L., Calcedo, R., Johnston, J., and Wilson, J. M. (2002). Novel adeno-associated viruses from rhesus monkeys as vectors for human gene therapy. *Proc. Natl. Acad. Sci. USA* 99: 11854–11859.
  42. Rabinowitz, J. E., et al. (2002). Cross-packaging of a single adeno-associated virus (AAV) type 2 vector genome into multiple AAV serotypes enables transduction with broad specificity. *J. Virol.* 76: 791–801.
  43. Veldwijk, M. R., et al. (2002). Development and optimization of a real-time quantitative PCR-based method for the titration of AAV-2 vector stocks. *Mol. Ther.* 6: 272–278.
  44. Kikuchi, T., et al. (1995). *Anat. Embryol. (Berlin)* 191: 101–118.

# Cerebrospinal Fluid Neprilysin is Reduced in Prodromal Alzheimer's Disease

Masahiro Maruyama, MD, PhD,<sup>1</sup> Makoto Higuchi, MD, PhD,<sup>1,2</sup> Yoshie Takaki, PhD,<sup>2</sup> Yukio Matsuba, BS,<sup>3</sup> Haruko Tanji, MD, PhD,<sup>1</sup> Miyako Nemoto, MD,<sup>1</sup> Naoki Tomita, MD,<sup>1</sup> Toshifumi Matsui, MD, PhD,<sup>1</sup> Nobuhisa Iwata, PhD,<sup>2</sup> Hiroaki Mizukami, MD, PhD,<sup>3</sup> Shin-ichi Muramatsu, MD, PhD,<sup>3</sup> Keiya Ozawa, MD, PhD,<sup>3</sup> Takaomi C. Saido, PhD,<sup>2</sup> Hiroyuki Arai, MD, PhD,<sup>1</sup> and Hidetada Sasaki, MD, PhD<sup>1</sup>

Amyloid  $\beta$  peptide (A $\beta$ ) has been implicated in Alzheimer's disease (AD) as an initiator of the pathological cascades. Several lines of compelling evidence have supported major roles of A $\beta$ -degrading enzyme neprilysin in the pathogenesis of sporadic AD. Here, we have shown a substantial reduction of cerebrospinal fluid (CSF) neprilysin activity (CSF-NEP) in patients with AD-converted mild cognitive impairment and early AD as compared with age-matched control subjects. The altered CSF-NEP likely reflects changes in neuronal neprilysin, since transfer of neprilysin from brain tissue into CSF was demonstrated by injecting neprilysin-carrying viral vector into the brains of neprilysin-deficient mice. Interestingly, CSF-NEP showed an elevation with the progression of AD. Along with a close association of CSF-NEP with CSF tau proteins, this finding suggests that presynaptically located neprilysin can be released into CSF as a consequence of synaptic disruption. The impact of neuronal damages on CSF-NEP was further demonstrated by a prominent increase of CSF-NEP in rats exhibiting kainate-induced neurodegeneration. Our results unequivocally indicate significance of CSF-NEP as a biochemical indicator to pursue a pathological process that involves decreased neprilysin activity and A $\beta$ -induced synaptic toxicity, and the support the potential benefits of neprilysin up-regulation in ameliorating neuropathology in prodromal and early AD.

Ann Neurol 2005;57:832–842

Numerous investigations have supported the contention that senile plaques and neurofibrillary lesions, composed primarily of amyloid  $\beta$  peptide (A $\beta$ ) and tau proteins, respectively, are not only descriptive characteristics of histopathology in brains with Alzheimer's disease (AD), but also mechanistically related to the pathogenesis of AD. That all of the genetic mutations causally linked to familial AD induce overproduction of either total A $\beta$  or relatively amyloidogenic A $\beta$ <sub>42</sub><sup>1</sup> further provides supportive evidence for the role of A $\beta$  accumulation as an initiator of the pathological cascade toward the onset of AD.<sup>2</sup>

The diagnosis of AD is definite based on magnitudes of these hallmark lesions after an autopsy, whereas exploitation of AD-specific biochemical markers reflecting central pathogenic processes, such as degeneration of neurites and synapses and alterations of A $\beta$  and tau, for antemortem diagnosis is still ongoing. Since 1995, two categories of cerebrospinal fluid (CSF) markers, CSF-tau and CSF-A $\beta$ <sub>42</sub>, have emerged and have

proved to be useful indicators to assist clinical diagnosis of AD in living patients.<sup>3–5</sup> Furthermore, several recent studies have demonstrated usefulness of CSF-tau in differentiation of prodromal AD from AD-unrelated cognitive decline among patients with mild cognitive impairment (MCI).<sup>6,7</sup> In contrast, altered processing of amyloid precursor protein and A $\beta$  has not been detected by biochemical markers such as CSF-A $\beta$ <sub>42</sub> in MCI patients,<sup>6</sup> although it is conceived to be upstream of tau abnormalities in the cascade of AD pathogenesis. Because therapeutic approaches, including existing drugs<sup>8</sup> and emerging treatments modifying A $\beta$  pathology,<sup>9,10</sup> presumably have the greatest potential of being effective in the prodromal phase of AD, accurate prediction of conversion to AD in patients with MCI by means of biological indices representing abnormal metabolism of amyloid precursor protein/A $\beta$  is particularly crucial. This gives us a rationale of analyzing accessible body fluid in search for altered levels of

From the <sup>1</sup>Department of Geriatric Medicine, Tohoku University School of Medicine, Sendai, Miyagi; <sup>2</sup>Laboratory for Proteolytic Neuroscience, RIKEN Brain Science Institute, Wako, Saitama; and <sup>3</sup>Division of Genetic Therapeutics, Center for Molecular Medicine, Jichi Medical School, Minamikawachi, Tochigi, Japan.

Received Oct 22, 2004, and in revised form Feb 23, 2005. Accepted for publication Mar 14, 2005.

Published online May 23, 2005 in Wiley InterScience (www.interscience.wiley.com). DOI: 10.1002/ana.20494

Address correspondence to Dr Higuchi, Laboratory for Proteolytic Neuroscience, RIKEN Brain Science Institute, 2-1 Hirosawa, Wako, Saitama 351-0198, Japan. E-mail: mhiguchi@brain.riken.jp

Table 1. Clinical Characteristics of Study Subjects (mean  $\pm$  SE)

Characteristic	Control	sMCI	pMCI	AD
No. of patients	27	5	33	32
Male/female ratio	7/19	5/0	10/13	9/23
Age (yr)	70.0 $\pm$ 1.5	74.4 $\pm$ 6.1	74.5 $\pm$ 1.0	73.1 $\pm$ 1.3
Years of education	10.8 $\pm$ 0.4	9.2 $\pm$ 0.1	11.7 $\pm$ 0.5	9.8 $\pm$ 0.9
MMSE score at baseline	28.6 $\pm$ 0.3	26.8 $\pm$ 0.8	25.3 $\pm$ 0.3	16.8 $\pm$ 1.0
Delayed recall score on WMS-R	95.0 $\pm$ 5.5	66.0 $\pm$ 4.3	58.5 $\pm$ 2.0	—
Years of follow-up	1.9 $\pm$ 0.1	1.9 $\pm$ 0.2	2.0 $\pm$ 0.4	1.3 $\pm$ 0.1
Changes in MMSE score by the end of follow-up	0.3 $\pm$ 0.1	-0.7 $\pm$ 0.3	-3.3 $\pm$ 0.4	-1.7 $\pm$ 0.6
Annual changes in MMSE score	0.14 $\pm$ 0.07	-0.39 $\pm$ 0.14	-1.74 $\pm$ 0.23	-1.48 $\pm$ 0.52

SE = standard error; sMCI = stable mild cognitive impairment; pMCI = progressive MCI; AD = Alzheimer's disease; MMSE = Mini-Mental State Examination; WMS-R = Wechsler Memory Scale-Revised.

molecules in close association with pathogenic A $\beta$  accumulation in the brain.

One notable feature of A $\beta$  metabolism is that it is a normal physiological process occurring in diverse cell types. Because there has been no overt evidence for an increased production of A $\beta$  in sporadic AD, the molecular mechanism of A $\beta$  degradation is of growing interest. The neutral endopeptidase neprilysin (EC 3.4.24.11) is one of the enzymes implicated in physiological A $\beta$  catabolism.<sup>11,12</sup> In neurons, it is localized primarily to the presynaptic terminals, with its ectodomain facing extracellular matrix,<sup>11,13</sup> and thus is capable of degrading extracellular A $\beta$  released from nerve ends. Recent genetic approaches using neprilysin-deficient mice have demonstrated the ability of neprilysin to cleave endogenous A $\beta$ .<sup>12,14</sup> Moreover, a decline of neprilysin levels has also been found in the brains of patients with early-stage sporadic AD,<sup>15</sup> suggesting critical roles played by reduced neprilysin activity in the incipient process of A $\beta$  accumulation.

The purpose of the study reported here was to assess applicability of monitoring neprilysin activities in CSF (CSF-NEP) and plasma (plasma-NEP) of patients with MCI and AD for prediction of clinical course and for gaining insights into molecular events early in A $\beta$  pathogenesis. The results showed a significant decrease of CSF-NEP, which developed to AD, in patients with MCI and in patients with mild AD, indicating usefulness of CSF-NEP assay as an informative clinical adjunct.

## Subjects and Methods

### Subjects

We studied 96 patients (mean age  $\pm$  standard error, 72.5  $\pm$  0.8 years) who underwent evaluations for memory disturbance at the Tohoku University Hospital Outpatient Clinic on Dementia. Clinical assessments by geriatricians and neuropsychological examinations, including Mini-Mental State Examination (MMSE) and Wechsler Memory Scale-Revised were performed for all patients, as described in detail previously.<sup>16</sup> Our established criteria<sup>16</sup> based on the current consensus<sup>17</sup> were used for diagnosis of amnesic MCI, and a

diagnosis of AD was made in accordance with the National Institute of Neurological and Communication Disorders-Alzheimer's Disease and Related Disorders Association criteria.<sup>18</sup> Consequently, 38 patients fulfilled the diagnostic criteria for amnesic MCI, 32 patients were diagnosed as having AD, and 26 patients were found to be cognitively normal at baseline investigation.

During the 2-year follow-up period, 33 of the patients with amnesic MCI progressed to AD and were thus classified into progressive MCI (pMCI). Five patients with amnesic MCI who showed unchanged or improved cognitive functions remained, and they were categorized as having stable MCI (sMCI). Twenty-eight patients with pMCI and all of the patients who were diagnosed as having AD at baseline were treated with a 5mg daily dose of donepezil hydrochloride.

At baseline examination, plasma and CSF samples were collected from each patient. CSF-tau was determined using a sandwich enzyme-linked immunosorbent assay designed for measurement of total tau (INNOTEST hTau antigen; Innogenetics, Gent, Belgium), as described elsewhere.<sup>4</sup> CSF-A $\beta$ 42 was also quantified with a specifically constructed sandwich enzyme-linked immunosorbent assay system.<sup>6</sup> The sample collection was performed after written informed consent was obtained from each participant or a family member. Demographic profiles of the patients examined in this study are summarized in Table 1.

### Plasma and Cerebrospinal Fluid Neprilysin Activity Assay

Before high-throughput analysis, neprilysin in CSF was identified by immunoblotting for a subset of CSF samples with antibody against human neprilysin (goat polyclonal; 1:400 dilution; Genzyme-TECHNE, Minneapolis, MN). Lysates of murine primary cortical neurons overexpressing human neprilysin<sup>19</sup> were used as control samples. Subsequently, CSF-NEP in all patients was fluorometrically assayed as thiorphan-inhibitable peptidase activity, based on the previously described protocol.<sup>14</sup> Briefly, a 20 $\mu$ l CSF sample was used for enzymatic cleavage of succinyl-Ala-Ala-Phe-AMC, with or without thiorphan, a specific inhibitor of neprilysin. Similarly, plasma-NEP was biochemically quantified by using 5 $\mu$ l plasma samples.

The application of fluorometric assay to CSF samples was

validated by examining correlation between intensity of immunoblotting signal and measured CSF-NEP. In addition, we assessed the specificity of CSF-NEP assay by immunodepleting CSF samples with antibody against human neprilysin (Genzyme-TECHNE; goat polyclonal) and protein G agarose slurry (Oncogene/Calbiochem, Cambridge, MA). Antibody against GABA<sub>A</sub> receptor  $\alpha_1$  subunit (Santa Cruz, Santa Cruz Biotechnology, CA; goat polyclonal) was also used as a control antibody for immunodepletion.

### *Biochemical Characterization of Cerebrospinal Fluid Neprilysin*

Cortical brain samples from autopsy-confirmed AD cases were homogenized with 4 volumes of 50mM tris(hydroxymethyl)aminomethane (Tris)-hydrochloride buffer (pH 7.6) containing 150mM sodium chloride (NaCl) and protease inhibitor cocktail and centrifuged at 200,000 $\times g$  for 20 minutes at 4°C. The resultant pellet was rehomogenized with 3 volumes of the above-mentioned buffer plus 1% Triton X-100 (Sigma Labs, St. Louis, MO) and centrifuged at 200,000 $\times g$  for 20 minutes at 4°C. The supernatant was then used for immunoblot analysis. CSF samples from the patients were processed with sodium dodecyl sulfate polyacrylamide gel electrophoresis Clean-Up Kit (Amersham Biosciences, Piscataway, NJ). Lysates of murine primary cortical neurons overexpressing human neprilysin<sup>19</sup> and recombinant protein corresponding to the extracellular domain of human neprilysin (Genzyme-TECHNE) were also used as control samples. In addition, aliquots of the protein samples were chemically deglycosylated by using trifluoromethanesulfonic acid.<sup>20</sup> The nondeglycosylated and deglycosylated protein samples (~10 $\mu$ g) were applied to immunoblotting with antibody against human neprilysin (Genzyme-TECHNE).

### *Animal Experiments*

To prove the transport of neuronal neprilysin from the brain into CSF, we assayed CSF-NEP in neprilysin-deficient mice after intrahippocampal injection of recombinant adeno-associated viral vector expressing human neprilysin (rAAV-NEP), which was prepared as described elsewhere.<sup>14</sup> Twelve neprilysin-deficient mice (generously provided by Dr C. Gerard, Harvard Medical School), aged 18 to 20 months, were injected with 0.6 $\mu$ l rAAV-NEP preparations (~1.3  $\times$  10<sup>10</sup> genome copies) into the bilateral dentate gyri of the hippocampus (stereotaxic coordinates: anteroposterior, 2.4mm; mediolateral, 2.0mm; and dorsoventral, 2.0mm). At 10 weeks after injection, the mice were anesthetized with pentobarbital, and CSF was isolated from the cisterna magna compartment under a dissecting microscope, based on the protocol by DeMattos and colleagues.<sup>21</sup> CSF samples (20–30 $\mu$ l from each mouse) were combined into three pooled volumes. After the collection of CSF, blood sampling was performed by cardiac puncture. The mice were then transcardially perfused with phosphate-buffered saline (PBS), and the hippocampi were dissected, homogenized with 9 volumes of 50mM Tris-hydrochloride buffer (pH 7.6) containing 150mM NaCl and EDTA-free protease inhibitor cocktail, and centrifuged at 200,000 $\times g$  for 20 minutes at 4°C. The resultant pellet was rehomogenized with 2 volumes of above-mentioned buffer plus 1% Triton X-100 and centrifuged at 200,000 $\times g$  for 20

minutes at 4°C. The supernatant was used as solubilized membrane fraction for biochemical analyses. For comparison, CSF, plasma, and hippocampal samples were also obtained from 12 wild-type and 12 neprilysin-deficient mice, aged 20 to 22 months, that were untreated. Plasma- and CSF-NEP were measured as described earlier, and a similar experimental procedure was applied to assay for hippocampal neprilysin activity by using 10 $\mu$ g protein in the membrane fraction. In the plasma and hippocampal analyses, 3 of 12 mice were randomly chosen in each study group, and samples from the selected mice were used for the assays. In addition, we also performed immunoblotting of neprilysin in pooled CSF samples using antimouse neprilysin antibody (Genzyme-TECHNE; goat polyclonal). Recombinant mouse neprilysin (Genzyme-TECHNE) was used as a control.

Because neprilysin in degenerating neurons can be released into CSF due to disruption of membrane structures to which neprilysin is anchored, CSF-NEP is likely to be affected by not only the level of brain neprilysin, but also the magnitude of neurodegeneration. Hence, we examined CSF-NEP in rats after low- and high-dose administrations of kainic acid (KA), an inducer of excitotoxic insults in the CNS neurons. At 7 weeks old, nine female Sprague-Dawley rats were divided into three groups. Rats in the control group were intraperitoneally injected with PBS, and the low- and high-dose KA groups underwent intraperitoneal administration of 10 and 50mg/kg KA dissolved in PBS, respectively. CSF and blood samples were collected in the control rats and rats treated with low-dose KA at 48 hours after injection as in the mouse experiment. All rats in the high-dose KA group exhibited a lethal status epilepticus within 5 hours of injection, and CSF and blood were sampled immediately after death of the animals. After CSF and blood collections, rats in all groups were transcardially perfused with PBS, and the brains were removed. The right hemisphere was fixed overnight with 4% paraformaldehyde in phosphate buffer (pH 7.4). Protein level and enzymatic activity of neprilysin in the CSF, plasma, and hippocampal samples were quantified by immunoblotting and fluorometric assay, respectively, as described earlier. We also analyzed levels of tau in CSF by immunoblotting with anti-tau antibody (Tau-1; mouse monoclonal; Chemicon, Temecula, CA). Before immunoblotting, albumin and IgG were removed from CSF preparations using a ProteoExtract Albumin/IgG Removal Kit (Calbiochem, San Diego, CA), followed by dephosphorylation of the samples using alkaline phosphatase (Sigma). For histochemical and immunohistochemical analyses, representative 10 $\mu$ m frozen sections of the right hemisphere were generated. Extents of excitotoxic insults and synaptic loss were investigated by immunofluorescence staining with antibodies against calpain-cleaved  $\alpha$ -spectrin (rabbit polyclonal)<sup>22</sup> and vesicular GABA transporter (117G4; rabbit polyclonal; Synaptic Systems GmbH, Goettingen, Germany), respectively. Amount of neprilysin was also examined by using antineprilysin antibody (56C6; mouse monoclonal; Novocastra Laboratories, Newcastle, United Kingdom). Immunostaining signals were amplified with a TSA-Direct kit (NEN Life Science Products, Boston, MA).

### *Statistical Analyses*

For group comparisons of clinical and biochemical variables, one-way analysis of variance was done, followed by Bonfer-

roni multiple comparison test. Correlations between two variables were tested by the *t* statistic.

## Results

### Reduction of Cerebrospinal Fluid Neprilysin Activity in Early Stages of Alzheimer's Disease Pathogenesis

In 11 CSF samples, a close correlation between intensity of neprilysin immunoblotting signal and measured

CSF-NEP was observed (Figs 1A, B). Moreover, CSF-NEP was substantially reduced by immunodepleting the samples with antineprilysin antibody (see Fig 1C). These findings justify the application of CSF-NEP assay to high-throughput analysis of CSF samples with sufficient specificity.

Quantified CSF-NEP in the control, pMCI, and AD groups is shown in Figure 1D. CSF-NEP was signifi-

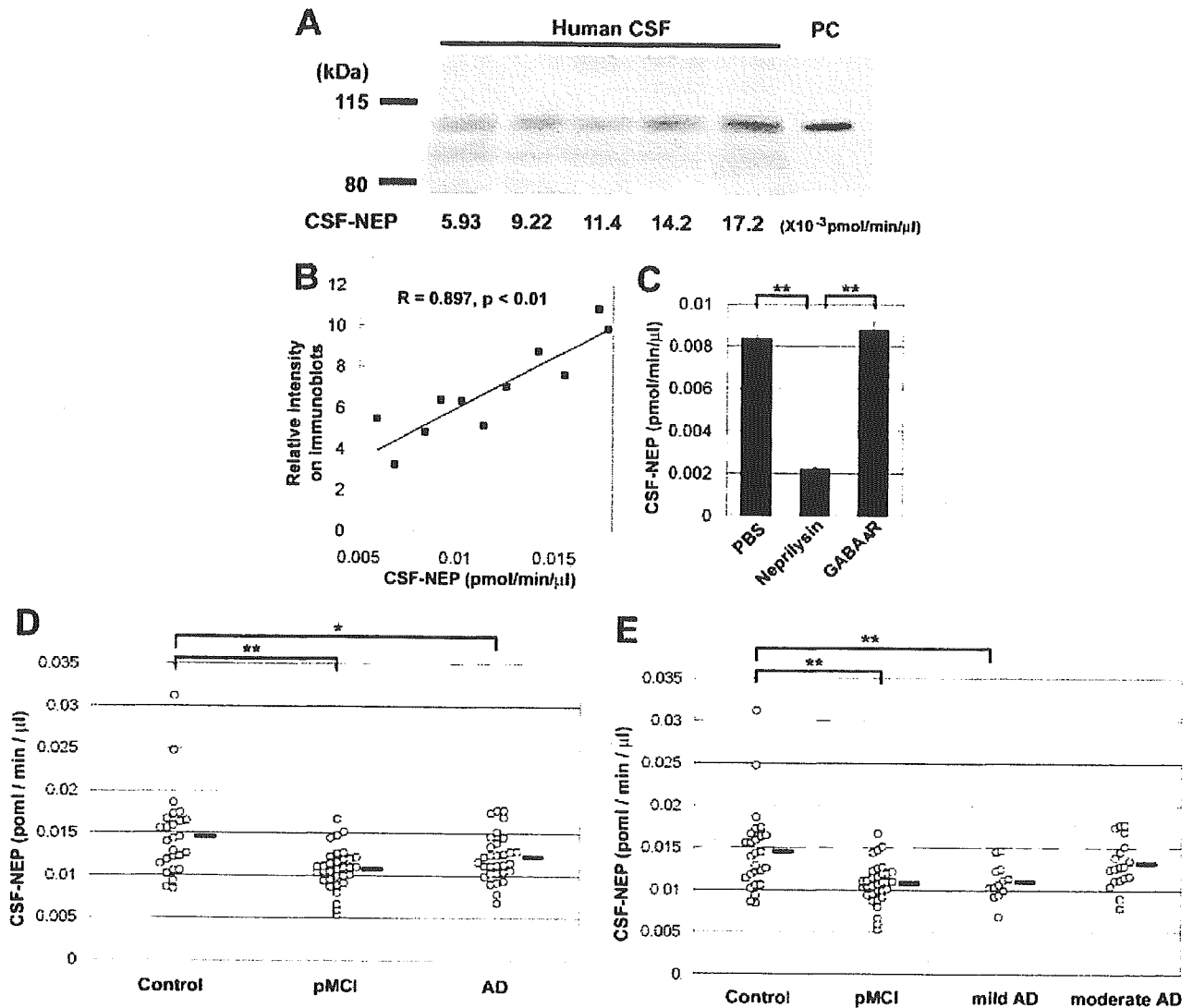


**Fig 1.** Decreased levels of cerebrospinal fluid neprilysin activity (CSF-NEP) in patients with incipient and mild Alzheimer's disease (AD). (A) Representative immunoblotting of neprilysin in human CSF samples demonstrates that apparent molecular mass of CSF neprilysin is nearly the same as that of the human neprilysin from primary culture (PC) of cortical neurons. The same volume of CSF preparation was loaded in each lane. CSF-NEP determined by fluorometric assay of enzymatic peptidolysis using the same sample is shown at the bottom. (B) CSF-NEP showed a close correlation with intensity of neprilysin immunoblotting signal in 11 human CSF samples. (C) CSF-NEP was reduced substantially by immunodepletion with antineprilysin antibody (neprilysin) relative to those in control subjects treated with either phosphate-buffered saline or antibody against anti-GABA<sub>A</sub> receptor  $\alpha_1$  subunit (GABA<sub>A</sub>R). All assays were performed in triplicate. Bars represent standard error. (D) A significant reduction of CSF-NEP was observed in patients with progressive mild cognitive impairment and AD compared with control subjects. Each circle represents the value obtained for a single individual, and horizontal lines represent the mean value in each group. (E) Patients with mild AD (Mini-Mental State Examination [MMSE] score, >17) showed a significant decline of CSF-NEP, whereas levels of CSF-NEP in patients with moderate AD (MMSE score, 9–17) were similar to those in control subjects. \**p* < 0.05; \*\**p* < 0.01.

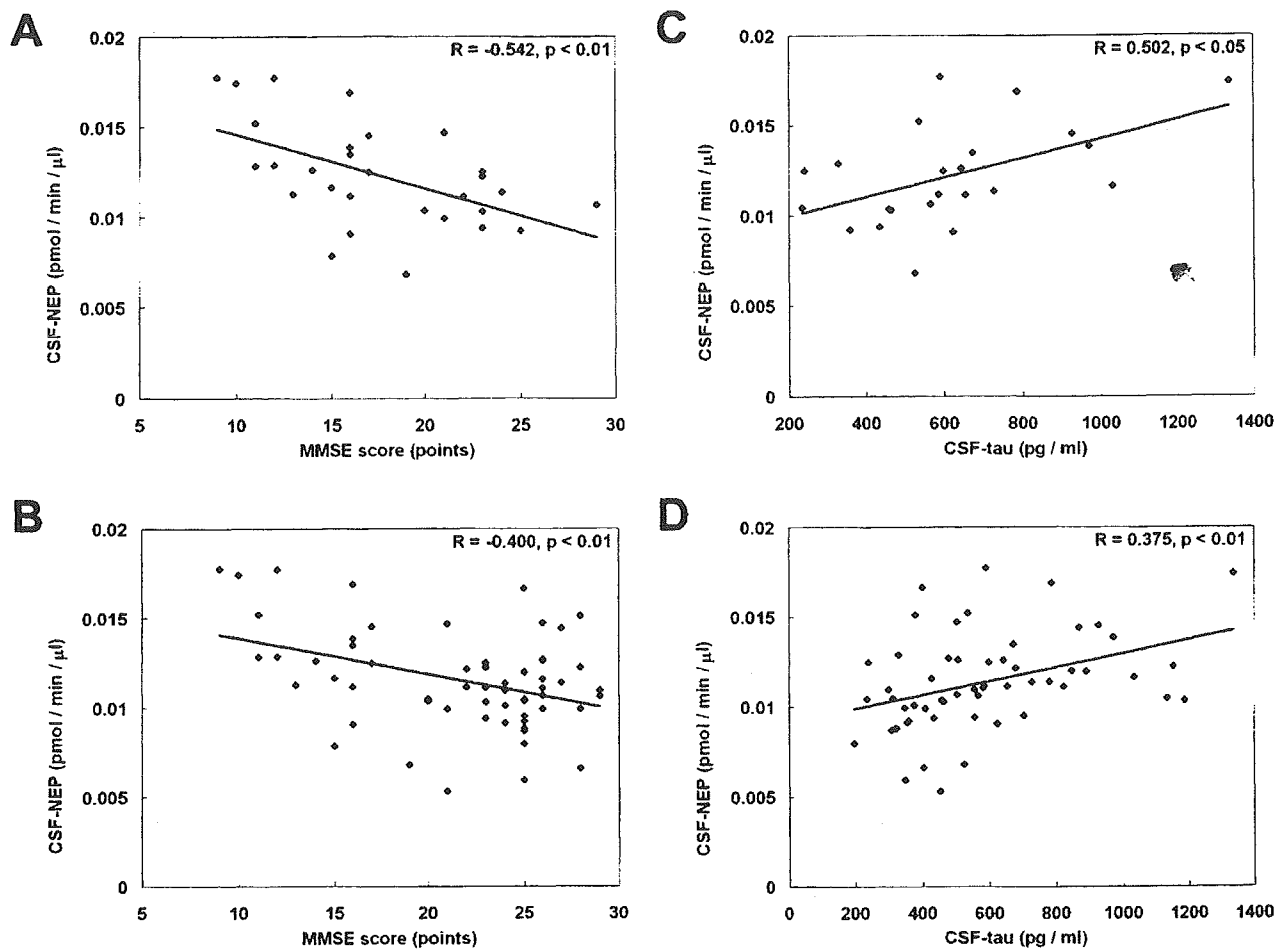


Fig 2. Association of cerebrospinal fluid neprilysin activity (CSF-NEP) (CSF-NEP) with disease severity assessed by Mini-Mental State Examination (MMSE) score and CSF-tau level in patients with progressive mild cognitive impairment (pMCI) and Alzheimer's disease (AD). (A) CSF-NEP was increased with disease progression in AD patients and was significantly correlated with MMSE score. (B) A significant correlation between CSF-NEP and MMSE score was also observed when patients with pMCI were added to the study group. (C) CSF-NEP showed a significant and positive correlation with CSF-tau in AD patients. (D) Correlation between CSF-NEP and CSF-tau levels remained significant when patients with pMCI were also included in the analysis. Solid lines represent the linear regression of the data.

cantly decreased in pMCI patients ( $0.0108 \pm 0.0004$  pmol/min/ $\mu$ l; mean  $\pm$  SE) compared with subjects in the control group ( $0.0146 \pm 0.0008$  pmol/min/ $\mu$ l). There also was a significant decrease of CSF-NEP in AD patients ( $0.0121 \pm 0.0005$  pmol/min/ $\mu$ l) compared with the control group. When the AD patients were subdivided into mild (MMSE scores, >17 points) and moderate AD groups (MMSE scores, 9–17 points), patients with mild AD showed a significant reduction of CSF-NEP ( $0.0107 \pm 0.0006$  pmol/min/ $\mu$ l) relative to the control subjects (see Fig 1E). By contrast, CSF-NEP in patients with moderate AD ( $0.0132 \pm 0.0007$  pmol/min/ $\mu$ l) was similar to the control level (see Fig 1E). Alteration of CSF-NEP during progression of AD was more intensively analyzed by plotting CSF-NEP data in AD patients against their MMSE scores. Notably, levels of CSF-NEP in AD patients showed a significant inverse

correlation with MMSE scores (Fig 2A). The correlation remained significant after data from pMCI patients were added to the plot (see Fig 2B). Thus, it is conceivable that occurrence of a prominent CSF-NEP reduction is confined to early stages of AD pathogenesis, and thereafter CSF-NEP is likely to be reversed to greater levels with advance of the disease.

AD patients with high levels of CSF-NEP showed higher levels of CSF-tau, thus the correlation between the two variables was significant (see Fig 2C). There also was a significant correlation between CSF-NEP and CSF-tau when patients with pMCI were combined with AD patients for analysis (see Fig 2D). Because CSF-tau is supposed to increase as a function of cytoskeletal disruption and abnormal tau accumulation in neurons, these findings support an increased diffusion of neuronal



neprilysin to the extracellular matrix and CSF as a consequence of injuries of neuronal membranes.

CSF-NEP was unrelated to CSF-A $\beta$ 42 in AD patients ( $R = -0.112$ ,  $p > 0.05$ ; data not shown), whereas correlation between these two variables became significant when patients with AD and pMCI were included for analysis ( $R = -0.262$ ,  $p < 0.05$ ; data not shown).

CSF-NEP was not correlated with age and sex in any of the studied groups. In addition to the aforementioned simple correlation analyses, multiple regression with stepwise selection option was used as an exploratory tool for identification of primary factors that determine levels of CSF-NEP in patients with pMCI and AD. As listed in Table 2, MMSE score and CSF-tau were selected as independent variables. CSF-tau showed the greatest partial correlation to CSF-NEP, and MMSE score also had a tendency to be correlated to CSF-NEP. Other variables, including age, sex, and CSF-A $\beta$ 42 were eliminated by the stepwise selection; thus, it is likely that the marked influence of the disease severity on both CSF-NEP and CSF-A $\beta$ 42 produced an apparent correlation between these two CSF measures in the simple correlation analysis.

CSF-NEP in sMCI subjects ( $0.0147 \pm 0.001$  pmol/min/ $\mu$ l) was similar to that in control subjects ( $p > 0.05$ ) and was significantly greater than that in pMCI subjects ( $p < 0.05$ ), implying applicability of CSF-NEP measurement to differentiation between pMCI and sMCI at baseline examination.

Neprilysin in CSF was further characterized by immunoblotting (Fig 3). Deglycosylated neprilysin in the brain and CSF showed the same molecular mass, which was larger than the apparent molecular weight of extracellular domain of neprilysin and corresponded to the predicted size of the full-length form. Therefore, secretion of neprilysin from neurons to the extracellular matrix likely occurs without shedding of the full-length enzyme.

Plasma-NEP did not differ among the control ( $1.669 \pm 0.306$  pmol/min/ $\mu$ l), pMCI ( $1.777 \pm$

Table 2. Multiple Regression Analysis for Patients with pMCI and AD

Independent Variable	Partial Correlation Coefficient	$p$
MMSE	-0.237	0.096
CSF-tau	0.292	0.042

$R^2 = 0.152$ ,  $F = 3.93$ ,  $p = 0.027$ .

Age, sex, and CSF-A $\beta$ 42 were eliminated from independent variables by the stepwise selection.

pMCI = progressive mild cognitive impairment; AD = Alzheimer's disease; MMSE = Mini-Mental State Examination; CSF = cerebrospinal fluid.

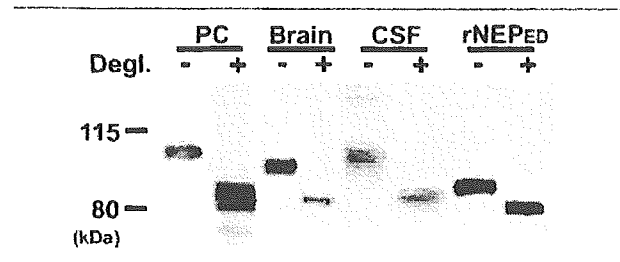
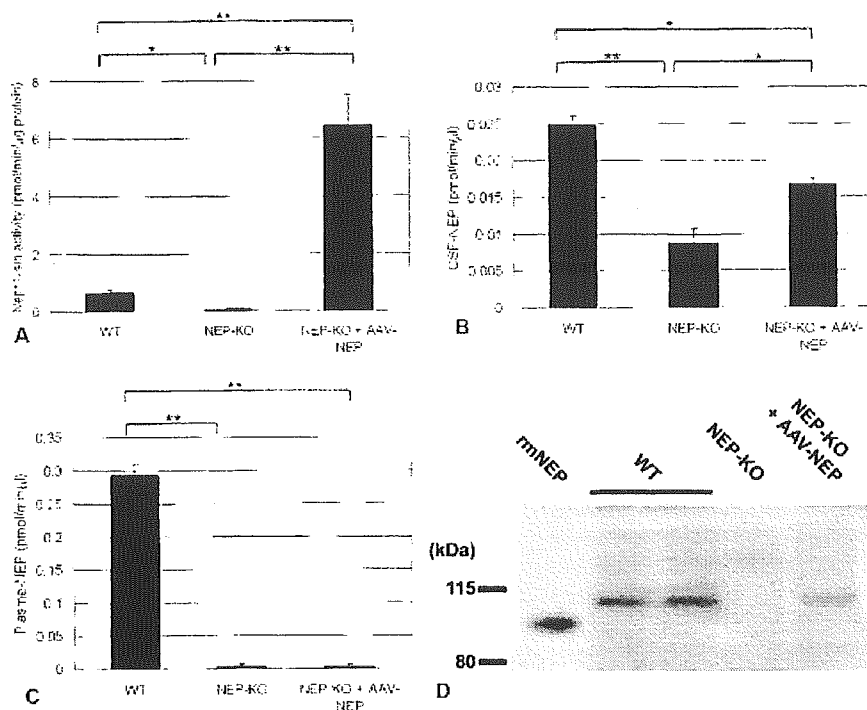


Fig 3. Biochemical characteristics of neprilysin in the brain and cerebrospinal fluid (CSF) from the human subjects. Non-deglycosylated neprilysin in the CSF sample from an AD patient migrated at approximately 95kDa, which was nearly the same as the apparent molecular mass of the human neprilysin from primary culture (PC) of cortical neurons, whereas neprilysin in the membrane-associated fraction extracted from the brain migrated slightly faster than the CSF neprilysin. After deglycosylation, the apparent molecular weight of neprilysin in the PC, brain, and CSF became approximately 85kDa, which corresponds to the predicted size of full-length, unmodified neprilysin. The recombinant extracellular domain of human neprilysin (rNEP<sub>ED</sub>) exhibited smaller apparent molecular mass than other samples.

$0.429$  pmol/min/ $\mu$ l), and AD ( $1.944 \pm 0.395$  pmol/min/ $\mu$ l) groups. Patients with mild ( $2.036 \pm 0.725$  pmol/min/ $\mu$ l) and moderate AD ( $1.816 \pm 0.494$  pmol/min/ $\mu$ l) exhibited similar levels of plasma-NEP. Moreover, there was no significant correlation between levels of CSF-NEP and plasma-NEP in any of the examined groups ( $R = 0.103$ ,  $p > 0.05$ ; data not shown). Hence, the CSF-NEP changes in patients with pMCI and early AD observed in this study were unrelated to the status of plasma neprilysin, but they conceivably reflected an altered transfer of neprilysin from the brain to CSF in these patients. This notion was further tested by the following experiments using rAAV-treated, neprilysin-deficient mice and KA-treated rats.

#### Physiological Transfer of Neprilysin from the Brain to Cerebrospinal Fluid Demonstrated in Mice

Neprilysin activity was assayed in the hippocampus, CSF, and plasma of neprilysin-deficient mice injected with rAAV-NEP, as well as untreated wild-type and neprilysin-deficient mice. Hippocampal neprilysin activity was nearly undetectable in the untreated neprilysin-deficient mice, whereas it prominently increased at 10 weeks after injection with rAAV-NEP (Fig 4A). There remained unnegligible signals in CSF-NEP assay for untreated neprilysin-deficient mice, which may be produced by degradation of the substrate by thiorphan semisensitive endopeptidases (see Fig 4B). In rAAV-NEP-treated, neprilysin-deficient mice, CSF-NEP showed a significant increase to approximately 70% of CSF-NEP in wild-type mice (see Fig 4B). By contrast, plasma-NEP in neprilysin-deficient mice treated with rAAV-NEP stayed at an undetectable level, similar to



**Fig 4.** Physiological transfer of neprilysin from the brain into CSF demonstrated by neprilysin-deficient mice injected with recombinant adeno-associated viral vector expressing human neprilysin (rAAV-NEP). (A) Hippocampal neprilysin activity was nearly undetectable in untreated neprilysin-deficient mice (NEP-KO). By contrast, NEP-KO mice at 10 weeks after intrahippocampal rAAV-NEP injection (NEP-KO + AAV-NEP) showed a pronouncedly high level of CSF-NEP, which was approximately 10-fold greater than the endogenous neprilysin activity in wild-type (WT) mice. (B) CSF samples of NEP-KO mice did not produce overt signals compared with those of WT mice. After administration of rAAV-NEP, CSF-NEP in NEP-KO mice was increased to 70% of the endogenous level in WT mice. (C) Unlike CSF-NEP, plasma-NEP did not display an apparent increase after treatment with rAAV-NEP. (D) Immunoblotting of neprilysin in mouse CSF showed consistency with CSF-NEP assay. Each lane was loaded with either CSF sample pooled from three mice or recombinant murine neprilysin (rmNEP). Bars represent standard error. \* $p < 0.05$ ; \*\* $p < 0.01$ .

untreated neprilysin-deficient mice (see Fig 4C). The transfer of neprilysin from the brains of rAAV-NEP-injected, neprilysin-deficient mice into CSF was also clearly demonstrated by immunoblotting of neprilysin in CSF samples (see Fig 4D). The predominance of the association between neprilysin activities in the brain and CSF over the plasma-CSF correlation suggests strong impacts of brain neprilysin activity on CSF-NEP through transfer of neuronal neprilysin into CSF in physiological conditions.

#### *Pathological Transfer of Neprilysin from the Brain to Cerebrospinal Fluid in Kainic Acid-Treated Rats*

In rats injected with KA, there was a KA-induced increase of CSF-NEP in a dose-dependent fashion; low-dose, KA-treated rats showed a slight and insignificant increase of CSF-NEP, and a pronounced increase in CSF-NEP (68-fold greater than the control level) was observed in rats treated with high-dose KA (Fig 5A). Unlike CSF-NEP, plasma-NEP did not significantly differ among the three groups (see Fig 5B). Immunoblotting of neprilysin also indicated a remarkable in-

crease of neprilysin in CSF samples from rats treated with high-dose KA (see Figs 5C [top panel], D [left panel]). In addition to neprilysin, levels of tau in CSF were prominently increased in rats injected with high-dose KA (see Figs 5C [bottom panel], D [right panel]). These data support an aberrantly increased transfer of both neprilysin and tau from damaged brain to CSF, providing a molecular basis for the close association between CSF-NEP and CSF-tau in patients with pMCI and AD (see Figs 2C, D).

Immunoblotting of neprilysin showed that neprilysin in membrane-associated protein fraction from the hippocampi was significantly reduced in rats injected with high-dose KA (Figs 6A, B [left panel]). Neprilysin in Tris/NaCl-soluble fraction had a tendency to increase in KA-treated rats in a dose-dependent fashion, although the increase was not statistically significant (see Figs 6A, B [right panel]). Immunohistochemistry for fragmented  $\alpha$ -spectrin indicated extensive activation of calpains in the entire hippocampus except the dentate gyrus after administration of KA at a high dose (see Figs 6C, D). A marked reduction of neprilysin immu-

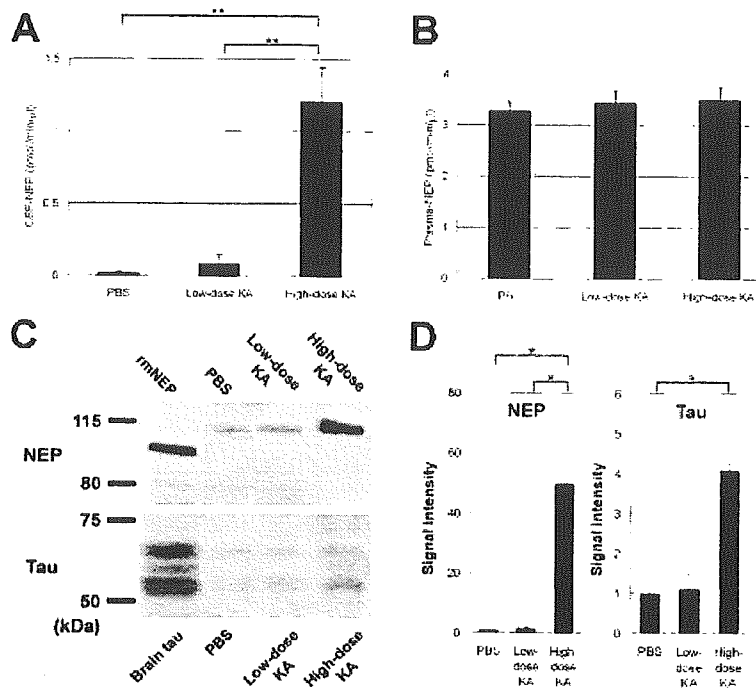


**Fig 5.** Increased transfer of neprilysin from the brain into cerebrospinal fluid (CSF) in a pathological condition as demonstrated by kainic acid (KA) challenge for rats. (A) Cerebrospinal fluid neprilysin activity (CSF-NEP) was increased after KA administration in a dose-dependent fashion. (B) Plasma-NEP did not significantly differ between rats injected with phosphate-buffered saline and KA. (C) Immunoblotting of neprilysin (top) also indicates a prominent increase of neprilysin in CSF from rats treated with high-dose KA. The CSF sample from a rat injected with high-dose KA was diluted fivefold, and equal volume was loaded in each lane. In addition to neprilysin, levels of tau proteins in CSF (bottom) were significantly increased in rats treated with high-dose KA. De-phosphorylated soluble fraction from rat brain tissue was applied as a control in tau immunoblotting. (D) Intensitometric data constituted from immunoblotting signals demonstrate significant increase in levels of NEP and tau in CSF from rats treated with high-dose KA. Bars represent standard error. \* $p < 0.05$ ; \*\* $p < 0.01$ .

noreactivity (see Figs 6E, F) accompanying loss of presynaptic signals in interneurons (see Figs 6G, H) was found in the hippocampal CA1 region of the rats treated with high-dose KA compared with the control rats (merged images are shown in Figs 6I, J). These results suggest that increased CSF-NEP in KA-treated rats can be caused by pathological transfer of neprilysin from surface of injured presynaptic membrane to CSF.

### Discussion

The principal outcome of this study was to demonstrate that CSF-NEP levels in patients with AD pathologies represent well both down-regulation of brain neprilysin early in the course of the aging-MCI-AD continuum and emanation of neprilysin from damaged neurons with exacerbation of the disease from early to intermediate stages. Importantly, decline of presynaptic neprilysin is putatively one of the earliest cytopathological events in AD pathogenesis<sup>23,24</sup> and is likely to intensify the local concentration of A $\beta$  in the vicinity of synaptic structures. As favored by circumstantial evidence,<sup>25</sup> accumulation of A $\beta$  may disrupt the integrity of synapses, conceivably causing further decrement of

presynaptically localized neprilysin. In light of our findings, we conclude that CSF-NEP is potentially an informative biochemical marker to monitor this vicious cycle of synaptic pathogenesis, which can accelerate an imbalance between neprilysin activity and A $\beta$  level in living patients with cognitive deficiency.

A literature of clinical studies has emerged indicating that CSF-tau assay permits prediction of AD-converted MCI and differentiation of prodromal AD from AD-unrelated MCI,<sup>6,7</sup> whereas persistent increase of CSF-tau at a nearly stable level regardless of disease stage<sup>26</sup> may hinder a chance to use CSF-tau as an antemortem index of neuropathological severity of AD. Unlike CSF-tau, CSF-A $\beta$ 42 is known to decline as the disease advances<sup>6</sup>; therefore, it may be useful to estimate magnitude of AD pathology in living patients. However, measurement of CSF-A $\beta$ 42 does not allow detection of abnormal A $\beta$  metabolism in prodromal AD because of a great overlap among normal, sMCI, and pMCI subjects.<sup>6,27</sup> Based on the data obtained in this study, CSF-NEP assay is capable of distinguishing pMCI patients from normal subjects with a sensitivity of 76% and a specificity of 74% when a cutoff threshold is

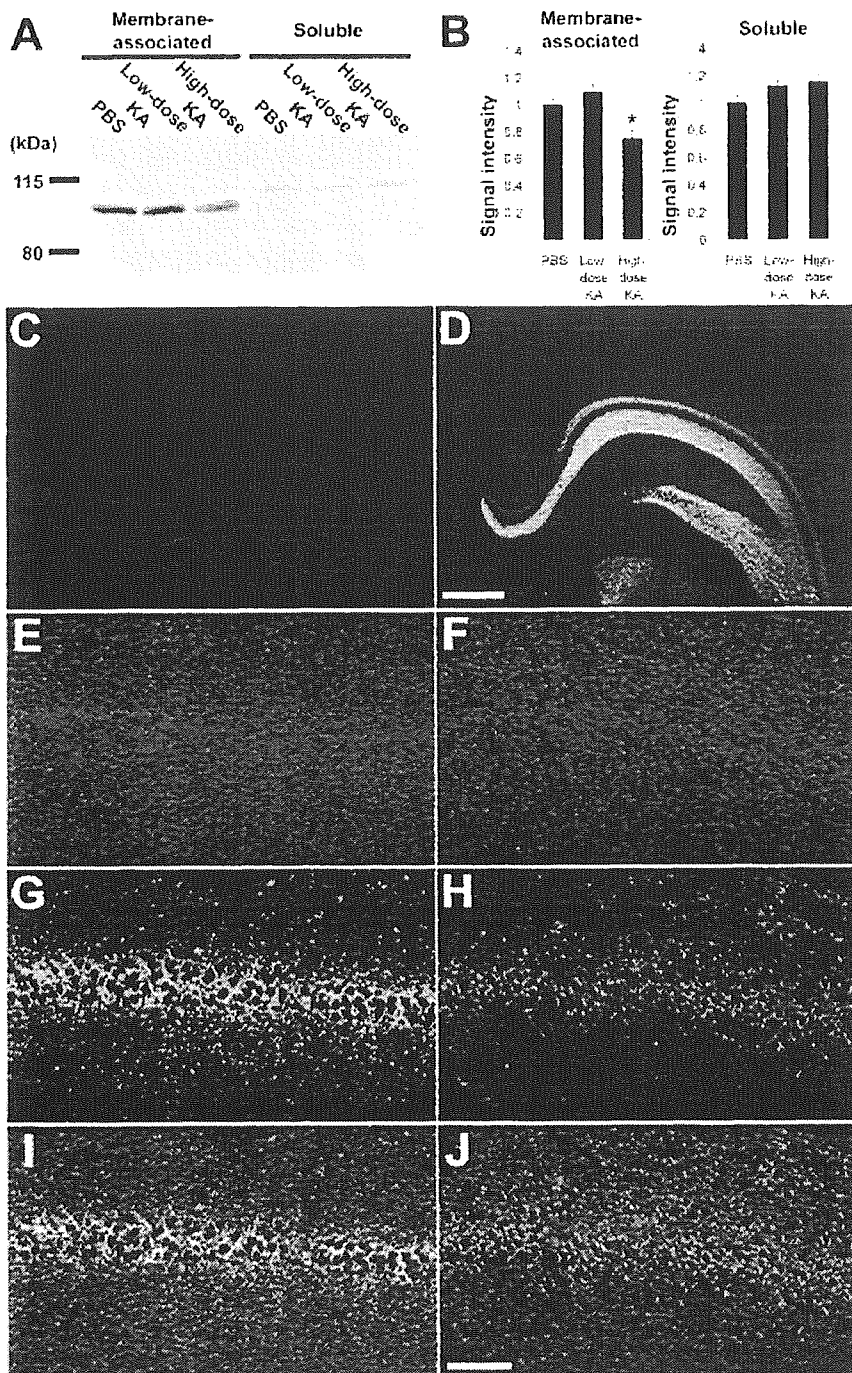


Fig 6. Reduction of neprilysin in disrupted presynaptic terminals observed in the hippocampal formations of rats treated with high-dose kainic acid (KA). (A) Representative immunoblotting indicates reduced level of membrane-associated neprilysin in high-dose KA group. Note that soluble neprilysin exhibits a larger molecular mass than membrane-associated neprilysin, presumably because of a higher magnitude of glycosylation. (B) Significant decrease of membrane-associated neprilysin in rats treated with high-dose KA was demonstrated by intensitometry of neprilysin immunoblotting signals. Bars represent standard error. (C–J) Immunostaining of hippocampal sections from rats treated with phosphate-buffered saline (left) and high-dose KA (right). Scale bars = 250 $\mu$ m (C, D); 100 $\mu$ m (E–J). \* $p < 0.05$ .

assigned at 0.012 pmol/min/ $\mu$ l. These values may not appear particularly impressive as compared with CSF-tau, but they clearly support feasibility of using CSF-

NEP as a valuable clinical adjunct to prediction of conversion from MCI to AD in view of A $\beta$  pathogenesis. Moreover, alteration of CSF-NEP as a function of dis-

ease severity enables evaluation of neuropathological progression as patients are longitudinally examined.

It should be noted that a reduction of CSF-NEP in pMCI is indicative of a decreased level of neuronal neprilysin and a consequent diminishment of physiological transfer of neprilysin from the brain to CSF. An increased level of CSF-NEP in neprilysin-deficient mice after intrahippocampal administration of rAAV-NEP has provided unequivocal evidence for such a transfer in nonpathological conditions. The molecular mechanisms by which neprilysin is released from healthy neurons to extracellular matrix remain to be elucidated. Our immunoblotting data indicate release of neprilysin from neurons without enzymatic shedding, unlike other membrane-bound metalloproteases.<sup>28,29</sup> Further biochemical assessments including mass spectrometric analysis of immunocaptured samples are required to identify membrane-unbound species of neprilysin that are transferable to CSF.

As mentioned earlier, the significant association of CSF-NEP with both MMSE score and CSF-tau suggests aberrant release of neprilysin from degenerating neurons. Because there was a lack of a significant correlation between CSF-tau and MMSE score in accordance with previous findings,<sup>26</sup> we postulate that diffusion of neprilysin from the central nervous system to CSF in neurodegeneration has primarily two distinct origins: neurons in the middle of active neuritic and synaptic disruptions, and neurons at the end stage of the degenerative process. Based on a marked and transient increase in CSF-tau levels after acute brain injuries,<sup>30,31</sup> CSF-tau levels supposedly reflect the number of neurons undergoing active degenerative processes. Diffusion of neprilysin from neurons to extracellular medium can first unfold on this acute and active neuropathology, as this experiment demonstrates using KA-treated rats. Neurons at the terminal stage of degenerative changes are unlikely to release a substantial quantity of tau, because tau in such neurons is depleted in the axonal compartment or is stuck to fibrillary aggregates in the somatodendritic compartment, or both.<sup>32</sup> However, advanced stages of cellular injury are presumed to still allow neurons to remain productive of neprilysin, and disruption or instability of membrane structures may promote emanation of neprilysin from these cells. The number of these terminally damaged neurons increases as the disease progresses, leading to an increase of CSF-NEP in tight association with disease severity.

Our data also suggest potential benefits of neprilysin up-regulation in treating patients with pMCI and mild AD and usefulness of CSF-NEP for biochemically evaluating efficacy of the treatment in these patients. In fact, suppression of A $\beta$  levels and amyloid plaque formation in amyloid precursor protein transgenic mice by genetically up-regulating neprilysin has been demonstrated by several independent groups.<sup>14,33,34</sup> Possi-

bility of pharmacological modulation of regulatory mechanisms for neprilysin activity has also been raised by various lines of supportive evidence.<sup>23,35</sup> CSF-NEP could have a predictive value for identifying who would be a responder to neprilysin activation among patients with pMCI and early-stage AD.

In conclusion, this study has provided strong clinical and experimental indication that compromised neprilysin activity, A $\beta$ -triggered neuronal injury, and a conjunction of these two changes in the brain can be monitored by CSF-NEP assay from predementia phase of AD. Quantification of CSF-NEP may also play a role in the diagnostic work-up of MCI to identify patients in transition from MCI to AD and patients afflicted by a depletion of brain neprilysin. This will be of particular importance when drugs with potential up-regulatory effects on neprilysin activity reach the clinical trial stage.

---

This work was supported by a grant from RIKEN BSI (M.H., Y.J., N.I., T.S.).

We thank Dr C. Gerard at Harvard Medical School for providing neprilysin-deficient mice and M. Sekiguchi for technical assistance. We appreciate the patients and their families who made our research possible through their generous efforts to foster research.

---

## References

1. Saido TC. A $\beta$  metabolism: from Alzheimer research to brain aging control. In: Saido TC, ed. A $\beta$  metabolism and Alzheimer's disease. Georgetown, TX: Landes Bioscience, 2003:1–16.
2. Hardy J, Selkoe DJ. The amyloid hypothesis of Alzheimer's disease: progress and problems on the road to therapeutics. *Science* 2002;297:353–356.
3. Motter R, Vigo-Pelfrey C, Kholodenko D, et al. Reduction of beta-amyloid peptide (42) in the cerebrospinal fluid of patients with Alzheimer's disease. *Ann Neurol* 1995;38:643–648.
4. Arai H, Terajima M, Miura M, et al. Tau in cerebrospinal fluid: a potential diagnostic marker in Alzheimer's disease. *Ann Neurol* 1995;38:649–652.
5. Growdon JH. Biomarkers of Alzheimer disease. *Arch Neurol* 1999;56:281–283.
6. Maruyama M, Arai H, Sugita M, et al. Cerebrospinal fluid amyloid beta(1-42) levels in the mild cognitive impairment stage of Alzheimer's disease. *Exp Neurol* 2001;172:433–436.
7. Okamura N, Arai H, Maruyama M, et al. Combined analysis of CSF tau levels and [<sup>123</sup>I]iodoamphetamine SPECT in mild cognitive impairment: implications for a novel predictor of Alzheimer's disease. *Am J Psychiatry* 2002;159:474–476.
8. Doody RS. Current treatments for Alzheimer's disease: cholinesterase inhibitors. *J Clin Psychiatry* 2003;64(suppl 9):11–17.
9. Dodel RC, Hampel H, Du Y. Immunotherapy for Alzheimer's disease. *Lancet Neurol* 2003;2:215–220.
10. Scarpini E, Scheltens P, Feldman H. Treatment of Alzheimer's disease: current status and new perspectives. *Lancet Neurol* 2003;2:539–547.
11. Iwata N, Tsubuki S, Takaki Y, et al. Identification of the major A $\beta$ <sub>1-42</sub>-degrading catabolic pathway in brain parenchyma: suppression leads to biochemical and pathological deposition. *Nat Med* 2000;6:143–150.
12. Iwata N, Tsubuki S, Takaki Y, et al. Metabolic regulation of brain A $\beta$  by neprilysin. *Science* 2001;292:1550–1552.

13. Fukami S, Watanabe K, Iwata N, et al. A $\beta$ -degrading endopeptidase, neprilysin, in mouse brain: synaptic and axonal localization inversely correlating with A $\beta$  pathology. *Neurosci Res* 2002;43:39–56.
14. Iwata N, Mizukami H, Shirotani K, et al. Presynaptic localization of neprilysin contributes to efficient clearance of amyloid-beta peptide in mouse brain. *J Neurosci* 2004;24:991–998.
15. Yasojima K, Akiyama H, McGeer EG, McGeer PL. Reduced neprilysin in high plaque areas of Alzheimer brain: a possible relationship to deficient degradation of beta-amyloid peptide. *Neurosci Lett* 2001;297:97–100.
16. Maruyama M, Matsui T, Tanji H, et al. Cerebrospinal fluid tau protein and periventricular white matter lesions in patients with mild cognitive impairment: implications for 2 major pathways. *Arch Neurol* 2004;61:716–720.
17. Petersen RC, Doody R, Kurz A, et al. Current concepts in mild cognitive impairment. *Arch Neurol* 2001;58:1985–1992.
18. McKhann G, Drachman D, Folstein M, et al. Clinical diagnosis of Alzheimer's disease: report of the NINCDS-ADRDA Work Group under the auspices of Department of Health and Human Services Task Force on Alzheimer's Disease. *Neurology* 1984;34:939–944.
19. Hama E, Shirotani K, Iwata N, Saido TC. Effects of neprilysin chimeric proteins targeted to subcellular compartments on amyloid beta peptide clearance in primary neurons. *J Biol Chem* 2004;279:30259–30264.
20. Edge AS. Deglycosylation of glycoproteins with trifluoromethanesulphonic acid: elucidation of molecular structure and function. *Biochem J* 2003;376:339–350.
21. DeMattos RB, Bales KR, Parsadanian M, et al. Plaque-associated disruption of CSF and plasma amyloid- $\beta$  (A $\beta$ ) equilibrium in a mouse model of Alzheimer's disease. *J Neurochem* 2002;81:229–236.
22. Saido TC, Yokota M, Nagao S, et al. Spatial resolution of fodrin proteolysis in postischemic brain. *J Biol Chem* 1993;268:25239–25243.
23. Saito T, Takaki Y, Iwata N, et al. Alzheimer's disease, neuropeptides, neuropeptidase, and amyloid-beta peptide metabolism. *Sci Aging Knowledge Environ* 2003;2003:PE1.
24. Saido TC, Nakahara H. Proteolytic degradation of A $\beta$  by neprilysin and other peptidases. In: Saido TC, ed. A $\beta$  metabolism and Alzheimer's disease. Georgetown, TX: Landes Bioscience, 2003:61–80.
25. Selkoe DJ. Alzheimer's disease is a synaptic failure. *Science* 2002;298:789–791.
26. Itoh N, Arai H, Urakami K, et al. Large-scale, multicenter study of cerebrospinal fluid tau protein phosphorylated at serine 199 for the antemortem diagnosis of Alzheimer's disease. *Ann Neurol* 2001;50:150–156.
27. Jensen M, Schroder J, Blomberg M, et al. Cerebrospinal fluid A $\beta$ 42 is increased early in sporadic Alzheimer's disease and declines with disease progression. *Ann Neurol* 1999;45:504–511.
28. Chubinskaya S, Mikhail R, Deutsch A, Tindal MH. ADAM-10 protein is present in human articular cartilage primarily in the membrane-bound form and is upregulated in osteoarthritis and in response to IL-1alpha in bovine nasal cartilage. *J Histochem Cytochem* 2001;49:1165–1176.
29. Osenkowski P, Toth M, Fridman R. Processing, shedding, and endocytosis of membrane type 1-matrix metalloproteinase (MT1-MMP). *J Cell Physiol* 2004;200:2–10.
30. Hesse C, Rosengren L, Vanmechelen E, et al. Cerebrospinal fluid markers for Alzheimer's disease evaluated after acute ischemic stroke. *J Alzheimers Dis* 2000;2:199–206.
31. Franz G, Beer R, Kampfl A, et al. Amyloid beta 1-42 and tau in cerebrospinal fluid after severe traumatic brain injury. *Neurology* 2003;60:1457–1461.
32. Higuchi M, Lee VM, Trojanowski JQ. Tau and axonopathy in neurodegenerative disorders. *Neuromolecular Med* 2002;2:131–150.
33. Marr RA, Rockenstein E, Mukherjee A, et al. Neprilysin gene transfer reduces human amyloid pathology in transgenic mice. *J Neurosci* 2003;23:1992–1996.
34. Leissring MA, Farris W, Chang AY, et al. Enhanced proteolysis of beta-amyloid in APP transgenic mice prevents plaque formation, secondary pathology, and premature death. *Neuron* 2003;40:1087–1093.
35. Saito T, Iwata N, Tsubuki S, et al. Somatostatin regulates brain amyloid  $\beta$  peptide, A $\beta$ <sub>42</sub>, through modulation of proteolytic degradation. *Nat Med* 2005;11:434–439.